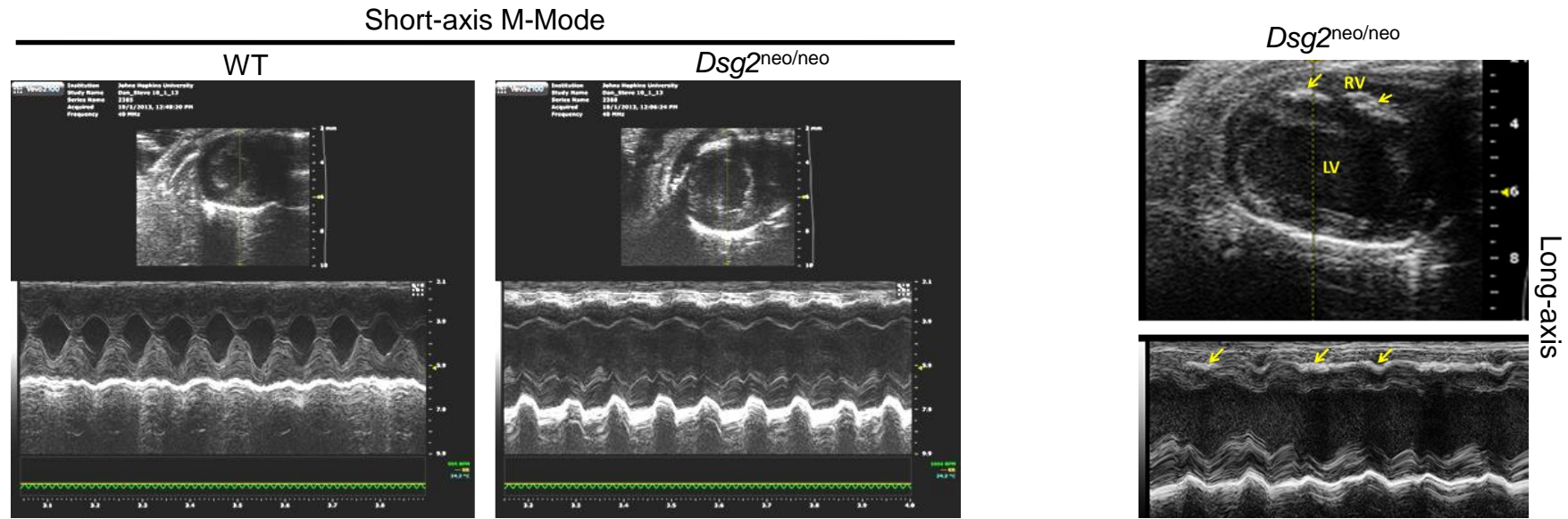
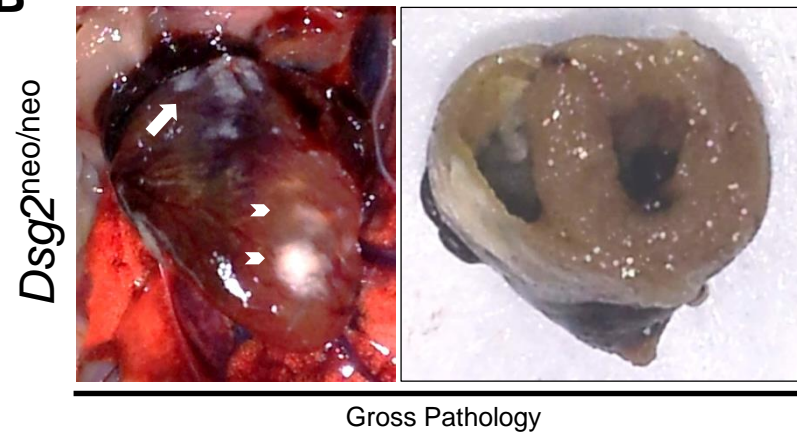
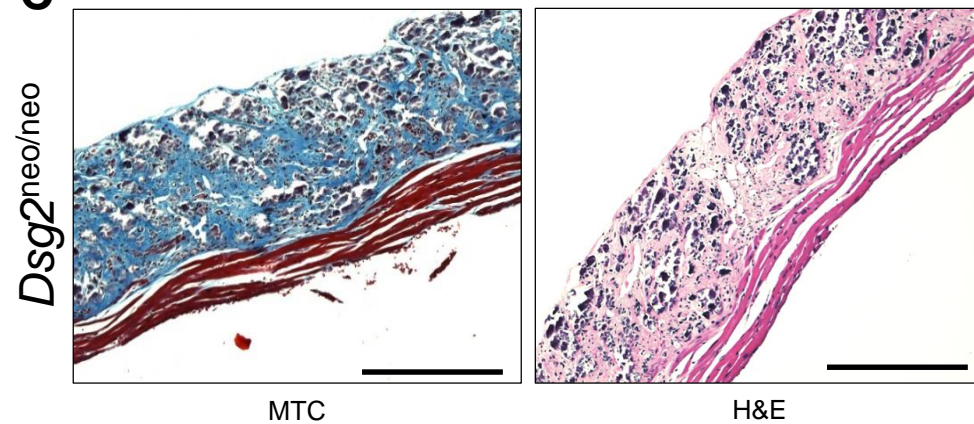
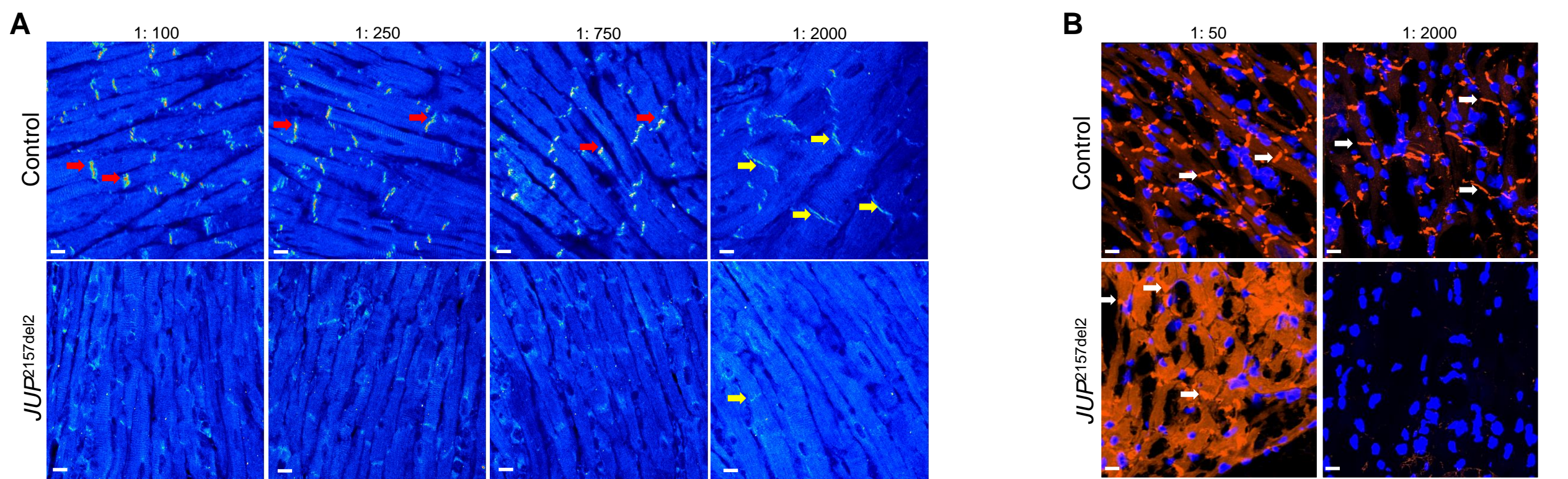
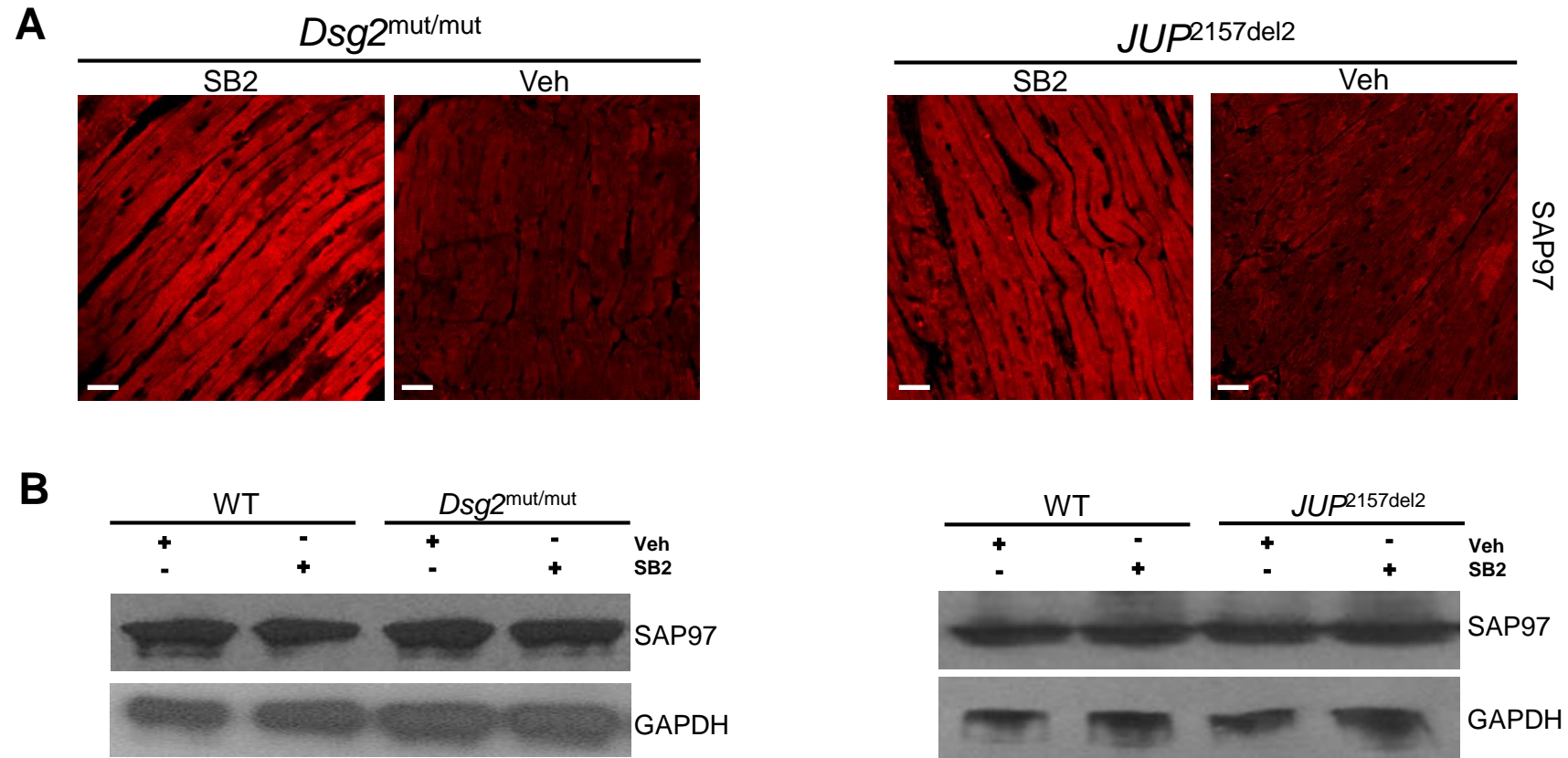


**A****B****C**

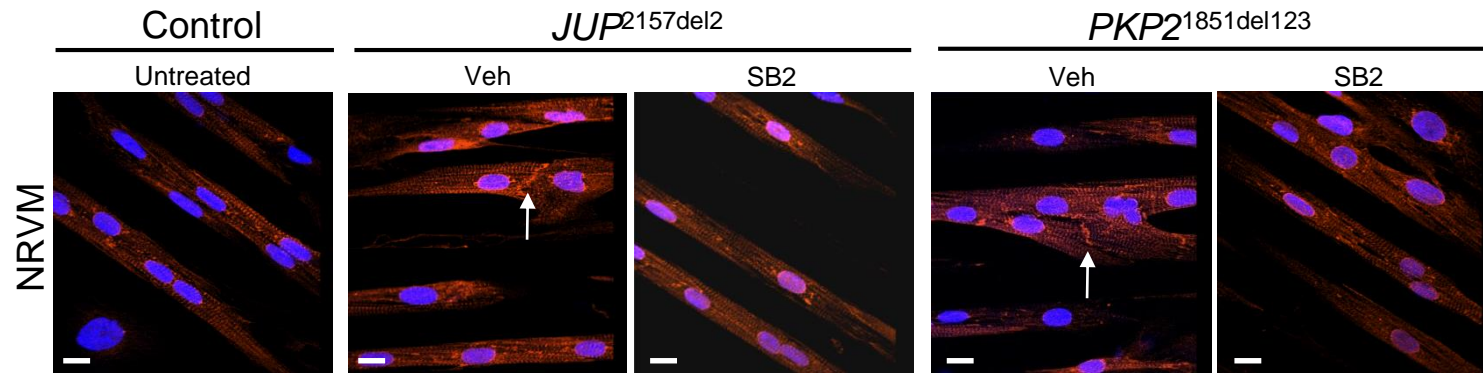
**Supplementary Figure 1. ACM disease phenotypes from *Dsg2<sup>neo/neo</sup>* mice at 16 weeks of age. (A)** Representative short-axis, m-mode and long-axis echocardiography from *Dsg2<sup>neo/neo</sup>* and WT mice. Yellow arrows; paradoxical septal wall motion with hypokinesia and fibrofatty deposits at antero-apical level; RV, right ventricle; LV, left ventricle;. **(B)** Gross pathology from *Dsg2<sup>neo/neo</sup>* mice. White arrow, RV outflow tract epicardial fibrosis; white arrowhead, LV epicardial and endocardial fibrosis. **(C)** RV myocardium stained for Masson's Trichrome (MTC) and H&E in *Dsg2<sup>neo/neo</sup>* mice. Scale bar: 100 $\mu$ m. Images are representative of n=4/genotype/parameter.



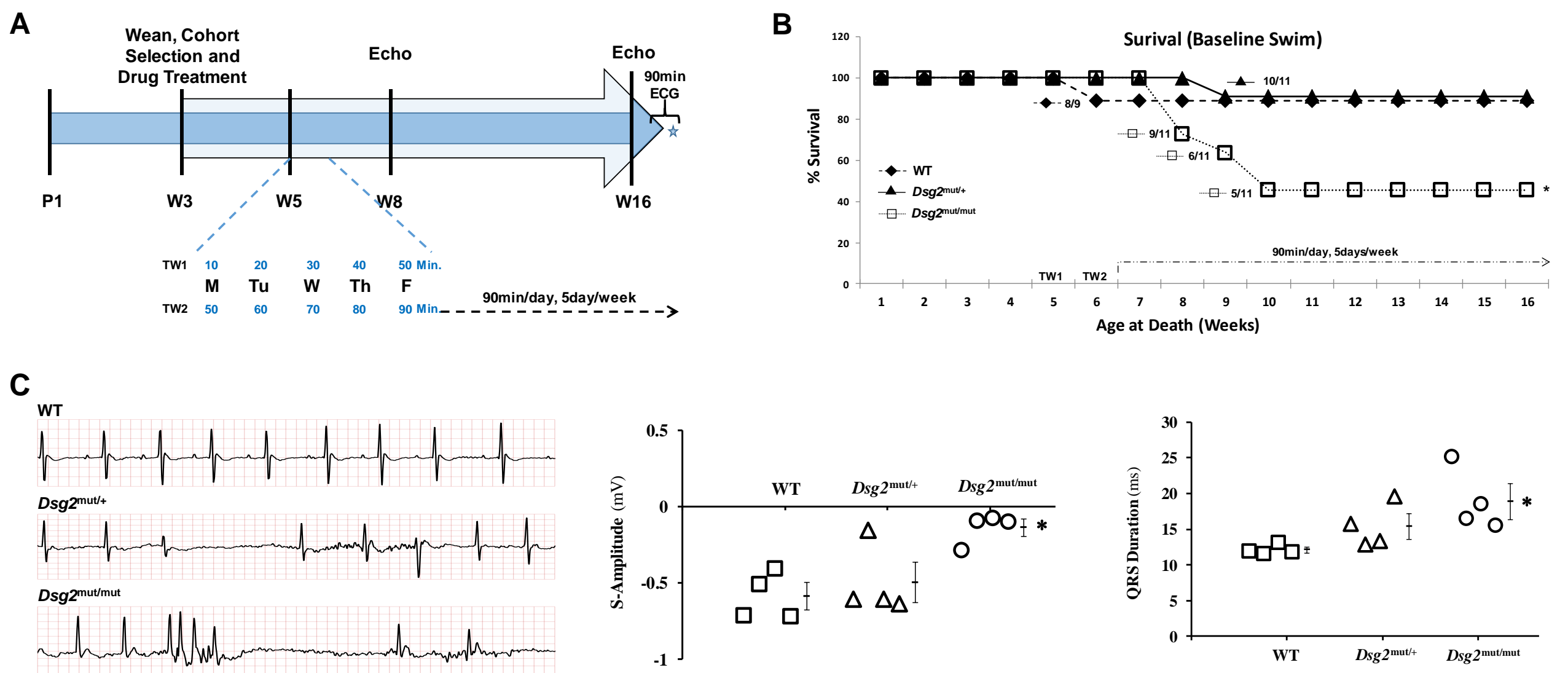
**Supplementary Figure 2. Plakoglobin immunostaining optimization.** (A) Formalin-fixed paraffin-embedded control and *JUP*<sup>2157del2</sup> mouse myocardium was immunolabeled for N-terminal directed anti-plakoglobin antibody (PLK-Nt) via serial dilution to obtain the optimal antibody concentration which demonstrated intercalated disc (ID) localization of PLK without hyper-saturation (red arrows). Serial dilution of PLK-Nt from control and *JUP*<sup>2157del2</sup> mouse myocardium reveals optimal concentration of antibody for ID signal (yellow arrows). Note, presence of PLK-Nt at IDs in *JUP*<sup>2157del2</sup> mice at a concentration of 1:2000, yet signal is considerably reduced compared to controls. Scale Bar: 10 $\mu$ m; anti-PLK-Nt from SIGMA. n=5 images/field from n=3 mice/genotype were utilized. (B) Snap-frozen myocardium from control and *JUP*<sup>2157del2</sup> mice shows ID signal for PLK-Nt (white arrows) from both genotypes at an antibody concentration of 1:50, however *JUP*<sup>2157del2</sup> mice displayed robust cytoplasmic localization. Optimal concentration of PLK-Nt was obtained at 1:2000 and showed complete absence of PLK-Nt signal in *JUP*<sup>2157del2</sup> mice myocardium. Scale Bar: 10 $\mu$ m; anti-PLK-Nt from Santa Cruz Biotechnology. n=5 images/field from n=3 mice/genotype were utilized.



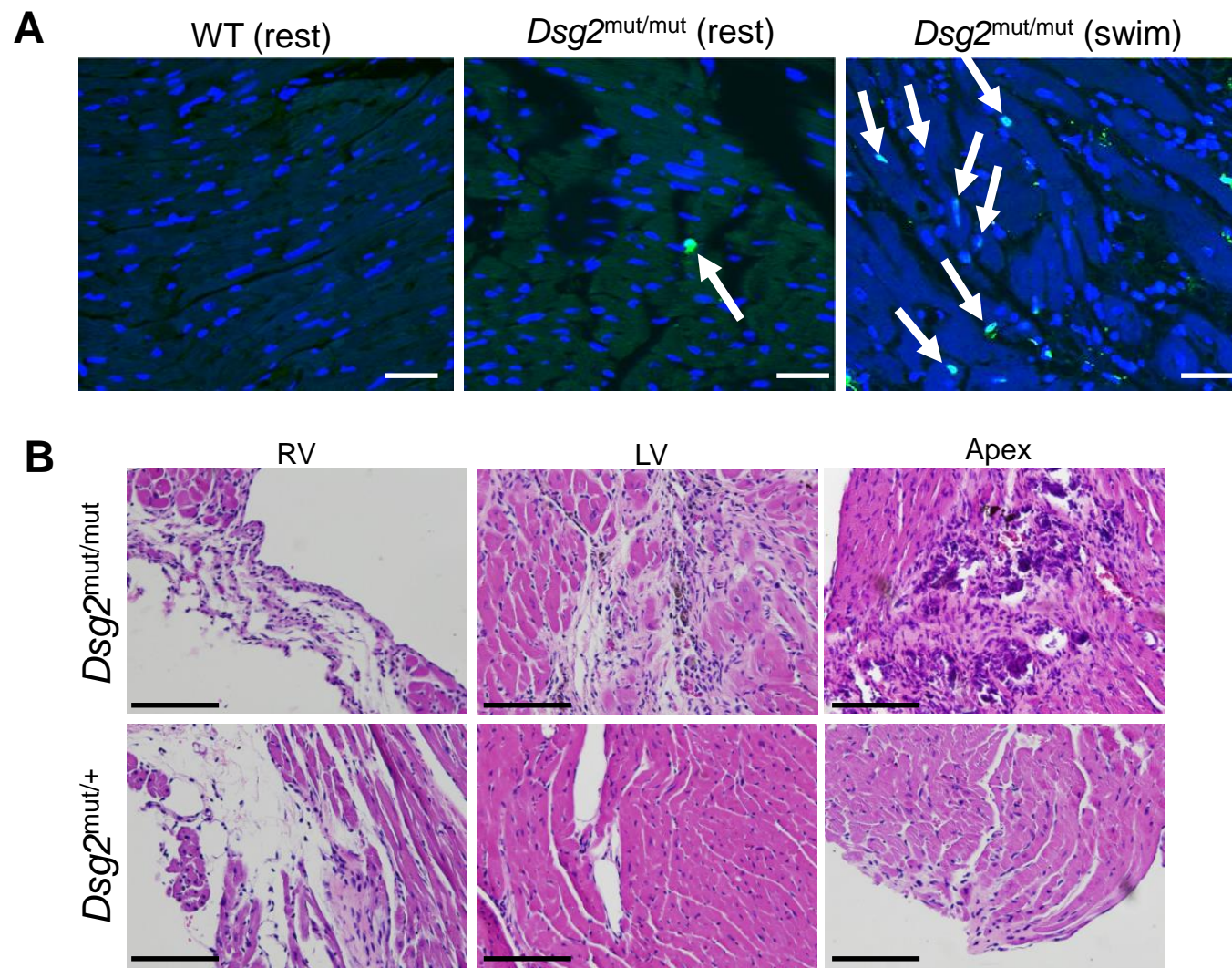
**Supplementary Figure 3. SB216763-treatment normalizes synapse associated protein 97 (SAP97) without apparent change in protein levels. (A)** Formalin-fixed, paraffin-embedded ventricular myocardium immunostained for SAP97 from WT and ACM mutant mice. Scale bar: 20 $\mu$ m. **(B)** Total cellular protein levels were probed for SAP97, normalized to GAPDH. Images are representative of n=4/genotype/treatment.



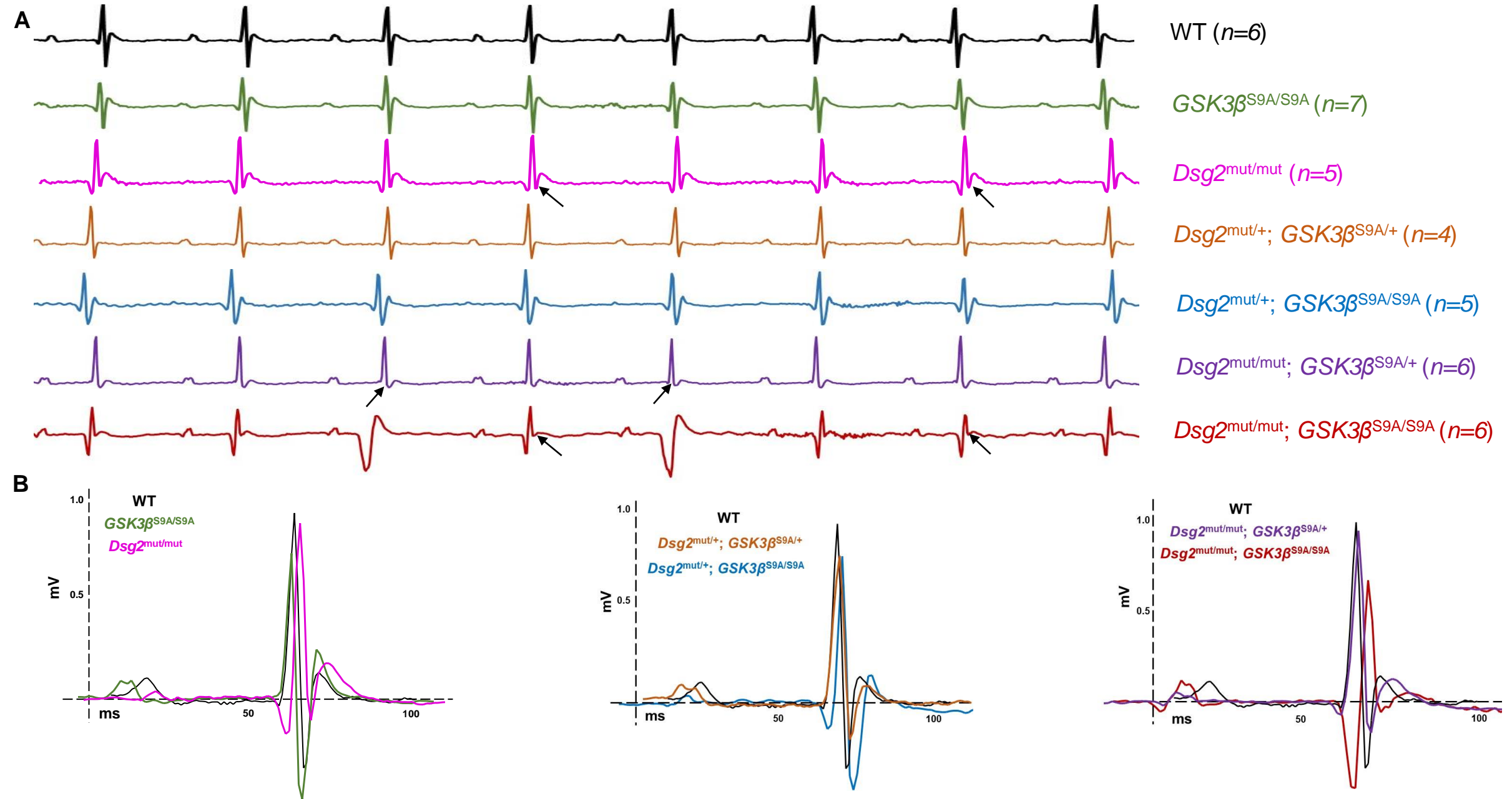
**Supplementary Figure 4. Accumulation of GSK3 $\beta$  immunosignal at the intercalated disc (ID) and reversal by SB216763 in engineered paired-myocytes.** Representative images of neonatal rat ventricular myocytes (NRVM) expressing *JUP*<sup>2157del2</sup> or *PKP2*<sup>1851del123</sup> transgenes grown on lines of fibronectin (width ~15 $\mu$ m), immunolabeled for GSK3 $\beta$  (red) and Dapi (blue). Scale bar: 10 $\mu$ m. White arrows, ID localization of GSK3 $\beta$ . Images are representative of n=3/genotype/treatment.



**Supplementary Figure 5. Percent survival and electrical abnormalities in baseline exercise studies.** (A) Schematic of exercise timeline. P1, postnatal day 1; TW1/TW2, training week 1/2; W3-W16, 3-16 weeks of age; M/Tu/W/Th/F, Monday-Friday; Blue star, timeline endpoint and tissue harvest following 16 week echocardiography (Echo) and 90min ECG recording. (B) Percent survival. mean±SEM, \*P<0.05 for *Dsg2<sup>mut/mut</sup>* vs WT using log-rank survival test. *n*-values inset, denominator is the total *n*-value for each genotype and the nominator is the *n*-value of survivors left during the course of the exercise study. (C) ECG telemetry tracings and parameters from exercised *Dsg2*-mutant and WT mice. mean±SEM, n=4/genotype, \*P<0.05 for *Dsg2<sup>mut/mut</sup>* vs WT using 2-tailed paired t-test.



**Supplementary Figure 6. Structural abnormalities in *Dsg2*-mutant mice from baseline exercise studies.** (A) TUNEL positive nuclei from sedentary (rest) WT and *Dsg2*<sup>mut/mut</sup> mice compared to baseline exercised (swim) *Dsg2*<sup>mut/mut</sup> mice. White arrows, TUNEL-positive nuclei. Images are representative of n=4/genotype. Scale bar: 20 $\mu$ m. (B) H&E stained myocardium from baseline exercised *Dsg2*<sup>mut/mut</sup> and *Dsg2*<sup>mut/+</sup> mice. RV, right ventricle; LV, left ventricle. Images are representative of n=4/genotype. Scale bar: 100 $\mu$ m



**Supplementary Figure 7. *Dsg2*-mutant mice with one or two copies of constitutively active GSK3 $\beta$ -S9A allele display ECG abnormalities.** (A) Representative ECG tracings from WT,  $GSK3\beta^{S9A/S9A}$ ,  $Dsg2^{mut/mut}$  and  $Dsg2$ -mutant mice with one or two copies of constitutively active GSK3 $\beta$ -S9A allele at 16 weeks of age. Black arrows highlight reduced S-Amplitude. (B) Single ECG tracings from WT and mutant mice. *n*-values are noted above.

	WT	<i>Dsg2</i> <sup>mut/mut</sup>
<b>Echocardiography</b>		
<i>n</i>	8	16
IVSd (mm)	0.90 ± 0.03	0.76 ± 0.03 ( <i>n</i> =15)
IVSs (mm)	1.44 ± 0.1	1.07 ± 0.1*
LVIDd (mm)	2.67 ± 0.1	3.09 ± 0.1*
LVIDs (mm)	1.07 ± 0.04	1.93 ± 0.2*
LVPWd (mm)	0.88 ± 0.04	0.9 ± 0.1
LVPWs (mm)	1.48 ± 0.04	1.26 ± 0.04* ( <i>n</i> =15)
FS (%)	59.9 ± 1.0	38.6 ± 3.8*
EF (%)	83.9 ± 0.8	60.3 ± 4.7*
<b>Morphometric</b>		
<i>n</i>	8	7
RWT (mm)	0.66 ± 0.04	0.73 ± 0.1 ( <i>n</i> =16)
LVM (mg)	9.34 ± 0.9	13.9 ± 1.4*
LVW/BW (mg/g)	0.42 ± 0.3	0.67 ± 0.1*
HW/BW (mg/g)	0.57 ± 0.03	0.68 ± 0.1

**Supplementary Table 1. Echocardiographic and morphometric indices from WT and *Dsg2*<sup>mut/mut</sup> mice at 8 weeks of age.** IVSd, interventricular septal end-diastolic volume; IVSs, interventricular septal end-systolic volume; LVIDd, left ventricular internal diameter end-diastolic volume; LVIDs, left ventricular internal diameter end-systolic volume; LVPWd, left ventricular posterior wall end diastole; LVPWs, left ventricular posterior wall end systole; FS, fractional shortening; EF, ejection fraction; RWT, relative wall thickness; LVM, left ventricular mass; LVW/BW, left ventricular weight to body weight; HW/BW, heart weight to body weight. mean±SEM, \*P<0.05 *Dsg2*<sup>mut/mut</sup> vs. WT using 2-way ANOVA with Tukey's post-hoc analysis. *n*-values are noted for all variables measured unless otherwise noted in italicized parentheses (*n*=X).



	WT		<i>Dsg2</i> <sup>mut/mut</sup>		<i>Dsg2</i> <sup>mut/+</sup>
	Sedentary	Swim	Sedentary	Swim	Swim
<b>Echocardiography</b>					
<i>n</i>	8	8	7	5	9
IVSd (mm)	0.91 ± 0.03	0.97 ± 0.02 <sup>†</sup>	0.78 ± 0.04 <sup>*</sup>	0.72 ± 0.1	1.03 ± 0.02 <sup>†</sup>
IVSs (mm)	1.51 ± 0.04	1.6 ± 0.04 <sup>†</sup>	1.05 ± 0.11 <sup>*</sup>	0.97 ± 0.17	1.54 ± 0.04 <sup>†</sup>
LVIDd (mm)	2.73 ± 0.09	2.8 ± 0.05 <sup>†</sup>	3.42 ± 0.31 <sup>*</sup>	3.9 ± 0.41	2.8 ± 0.05 <sup>†</sup>
LVIDs (mm)	1.08 ± 0.06	1.09 ± 0.03 <sup>†</sup>	2.54 ± 0.41 <sup>*</sup>	2.76 ± 0.6	1.05 ± 0.03 <sup>†</sup>
LVPWd (mm)	0.88 ± 0.05	0.93 ± 0.01	0.87 ± 0.05	0.85 ± 0.06	0.98 ± 0.04 <sup>†</sup>
LVPWs (mm)	1.54 ± 0.04 <sup>‡</sup>	1.64 ± 0.03 <sup>†</sup>	1.22 ± 0.05 <sup>*</sup>	1.24 ± 0.13	1.63 ± 0.04 <sup>†</sup>
FS (%)	60.6 ± 1.25	61.7 ± 0.6 <sup>†</sup>	27.8 ± 4.5 <sup>*</sup>	31.7 ± 8.6	62.6 ± 0.56 <sup>†</sup>
EF (%)	84.4 ± 1.0	85.3 ± 0.46 <sup>†</sup>	46.8 ± 7.0 <sup>*</sup>	51.0 ± 11.0	86.0 ± 0.43 <sup>†</sup>
<b>Morphometric</b>					
<i>n</i>	8	8	7	5	9
RWT (mm)	0.65 ± 0.05	0.66 ± 0.02	0.53 ± 0.05	0.68 ± 0.13	1.17 ± 0.04 <sup>†</sup>
LVM (mg)	9.8 ± 1.2	11.0 ± 0.09	13.6 ± 1.9	14.4 ± 2.6	12.6 ± 1.5
LVW/BW (mg/g)	0.44 ± 0.04 <sup>‡</sup>	0.53 ± 0.03	0.65 ± 0.09 <sup>*</sup>	0.68 ± 0.11	0.61 ± 0.07
HW/BW (mg/g)	0.58 ± 0.02	0.6 ± 0.02	0.68 ± 0.06	0.61 ± 0.04	0.63 ± 0.05

**Supplementary Table 2. Echocardiographic and morphometric indices from Vehicle-treated sedentary and exercised (Swim) mice at 16 weeks of age.** IVSd, interventricular septal end-diastolic volume; IVSs, interventricular septal end-systolic volume; LVIDd, left ventricular internal diameter end-diastolic volume; LVIDs, left ventricular internal diameter end-systolic volume; LVPWd, left ventricular posterior wall end diastole; LVPWs, left ventricular posterior wall end systole; FS, fractional shortening; EF, ejection fraction; RWT, relative wall thickness; LVM, left ventricular mass; LVW/BW, left ventricular weight to body weight; HW/BW, heart weight to body weight. mean±SEM, P<0.05 for <sup>\*</sup>*Dsg2*<sup>mut/mut</sup> (Sedentary) vs. WT (Sedentary); <sup>†</sup>WT and <sup>†</sup>*Dsg2*<sup>mut/+</sup> (Swim) vs. *Dsg2*<sup>mut/mut</sup> (Swim); and <sup>‡</sup>WT (Sedentary) vs. WT (Swim) using 2-way ANOVA with Tukey's post-hoc analysis. *n-values* noted above.

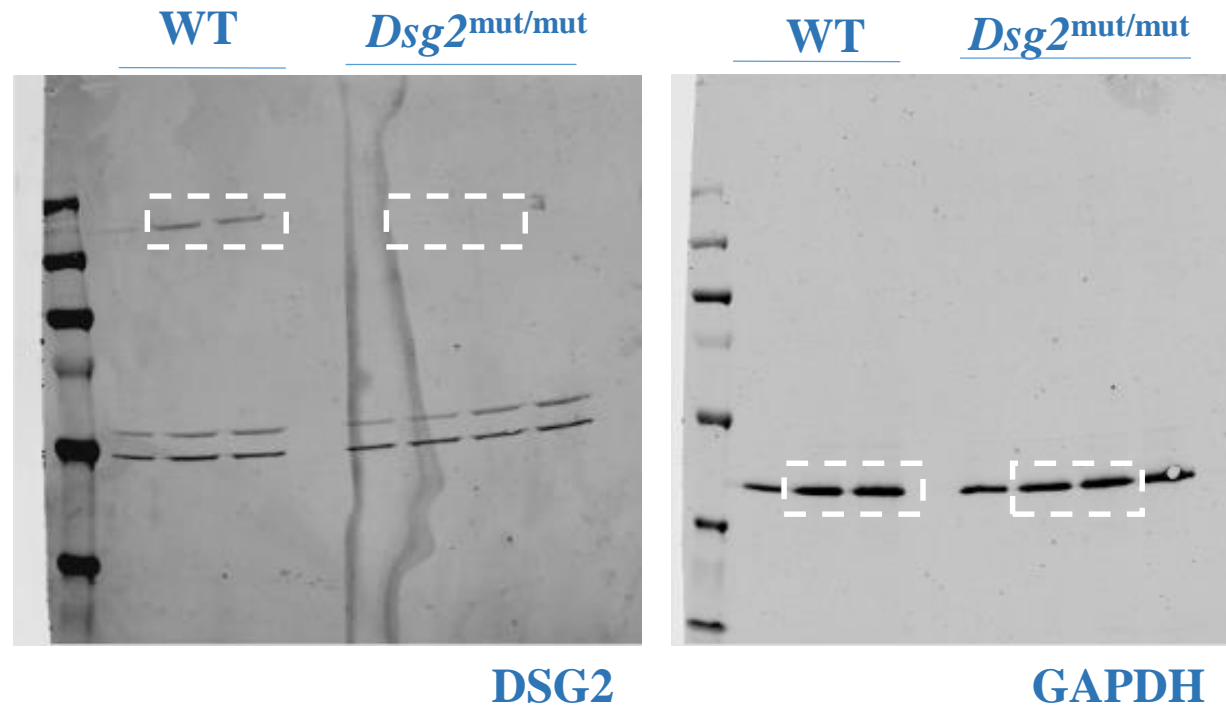
	WT	<i>GSK3β</i> <sup>S9A/S9A</sup>	<i>Dsg2</i> <sup>mut/mut</sup>	<i>Dsg2</i> <sup>mut/+</sup>		<i>Dsg2</i> <sup>mut/mut</sup>	
				<i>GSK3β</i> <sup>S9A/+</sup>	<i>GSK3β</i> <sup>S9A/S9A</sup>	<i>GSK3β</i> <sup>S9A/+</sup>	<i>GSK3β</i> <sup>S9A/S9A</sup>
<b>Electrocardiography</b>							
<i>n</i>	6	7	5	4	5	6	6
PR-I (ms)	33.0 ± 0.8‡	40.5 ± 2.0*†	32.8 ± 2.7‡	42.6 ± 1.5*†	39.6 ± 1.8*†	40.6 ± 2.0*†	40.2 ± 1.4*†
Pd (ms)	9.7 ± 0.8	8.8 ± 0.8	9.01 ± 2.1	11.9 ± 0.9‡	9.4 ± 1.5	10.9 ± 0.7‡	10.7 ± 1.1
P-Amp (mV)	0.06 ± 0.01††	0.04 ± 0.01*	0.03 ± 0.01*	0.09 ± 0.01††	0.05 ± 0.01	0.05 ± 0.01	0.05 ± 0.004
QRSd (ms)	11.4 ± 0.5†	12.4 ± 0.9	14.3 ± 1.3*	14.2 ± 1.6*	13.8 ± 0.69*	14.2 ± 0.66*	14.5 ± 0.9*
Q-Amp (mV)	-0.02 ± 0.01†	-0.02 ± 0.01†	-0.11 ± 0.03*‡	-0.02 ± 0.01†	-0.04 ± 0.01†	-0.04 ± 0.02†	-0.13 ± 0.05*‡
S-Amp (mV)	-0.36 ± 0.08†	-0.22 ± 0.07†	-0.03 ± 0.02*‡	-0.19 ± 0.07†	-0.24 ± 0.05†	-0.09 ± 0.06*	-0.06 ± 0.03*‡

**Supplementary Table 3. Electrocardiographic indices from 16 week old WT, *GSK3β*<sup>S9A/S9A</sup>, *Dsg2*<sup>mut/mut</sup> and *Dsg2*-mutant mice with one or two copies of constitutively active *GSK3β*-S9A.** PR-I, PR-Interval; Pd, P duration; P-Amp, P-Amplitude; QRSd, QRS duration; Q-Amp, Q-Amplitude; S-Amp, S-Amplitude. Data presented as mean±SEM, *n-values* noted above, with a P<0.05 deemed significant using 2-way ANOVA with Tukey's post hoc analysis. \*All groups vs. WT; †All groups vs. *Dsg2*<sup>mut/mut</sup>; ‡All groups vs. *GSK3β*<sup>S9A/S9A</sup>.

# Unedited Gels

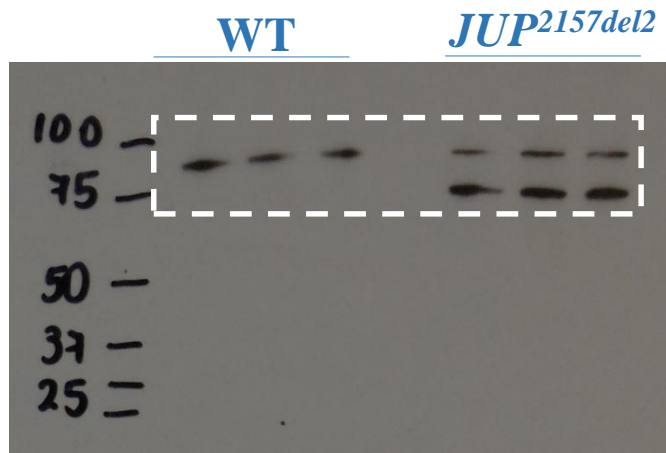
Lanes of the unedited gels which correspond to those shown within the manuscript have a dashed white box surrounding them.

# Full unedited gels for **Figure 2A**

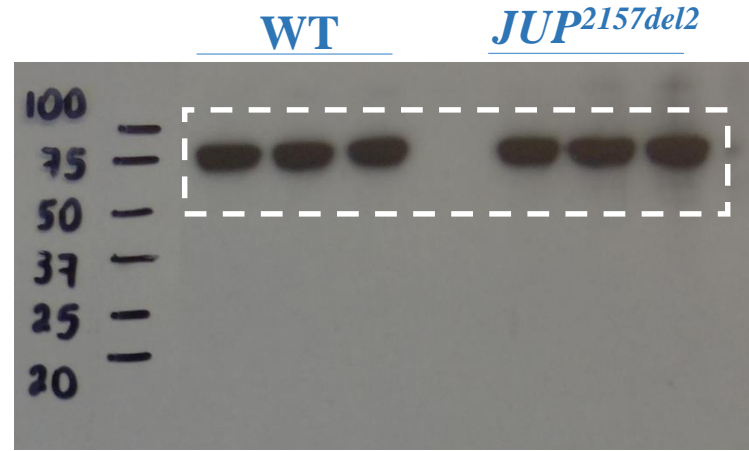


**16 Weeks of Age (NO Vehicle, NO SB216763)**

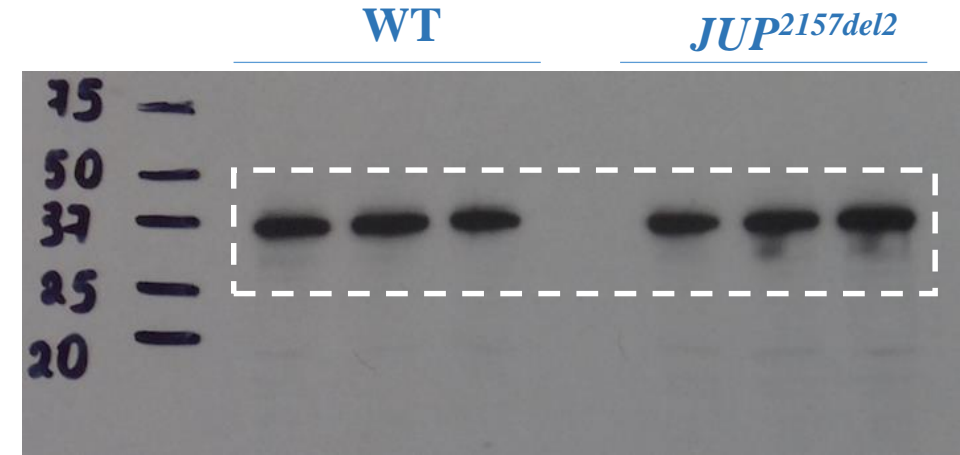
# Full unedited gels for **Figure 3A**



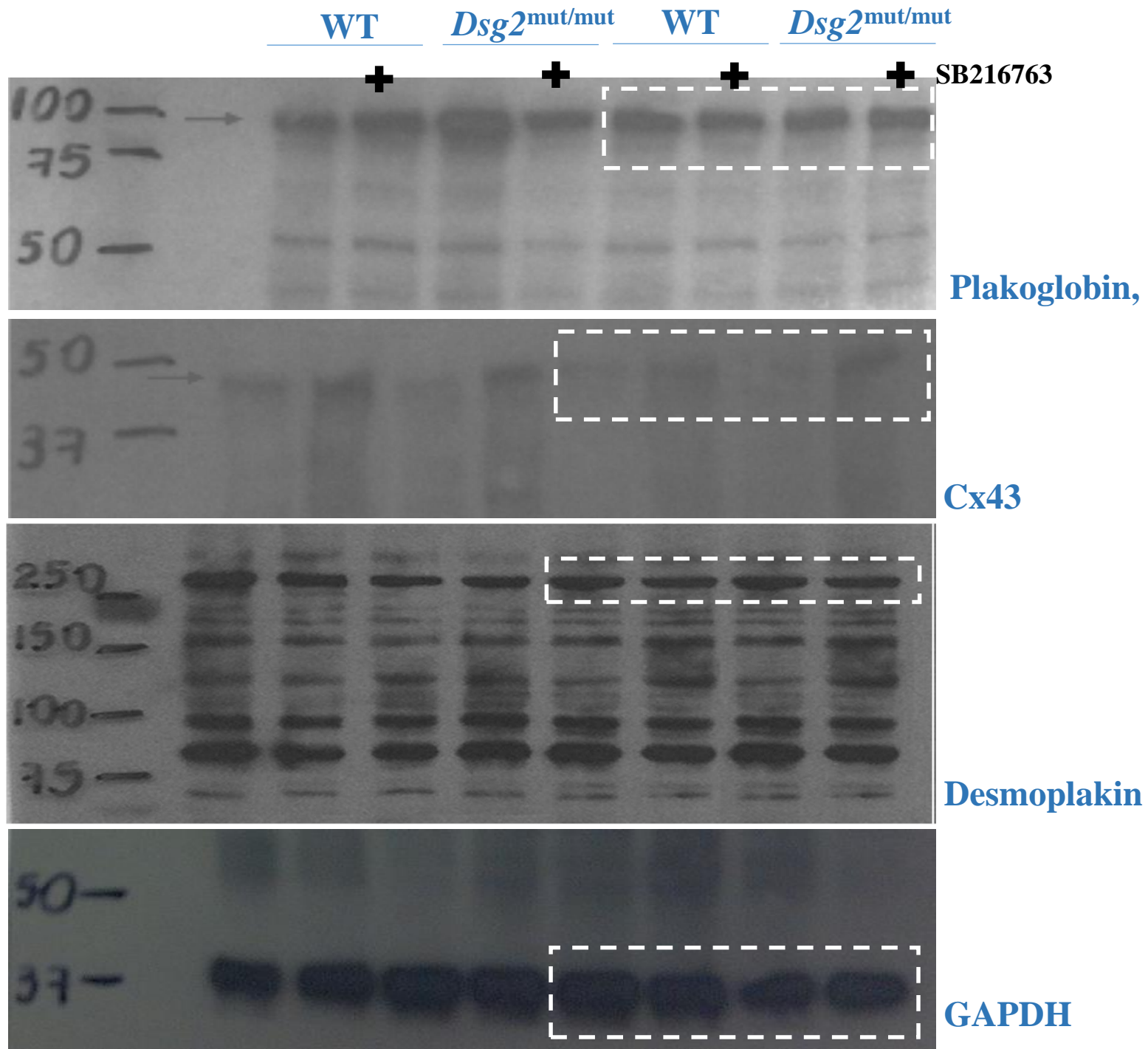
**Plakoglobin (N-term)**



**Plakoglobin (C-term)**

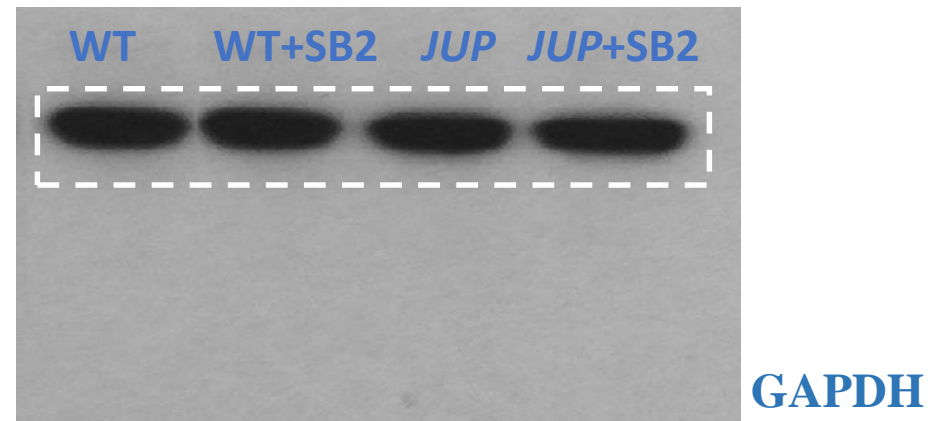
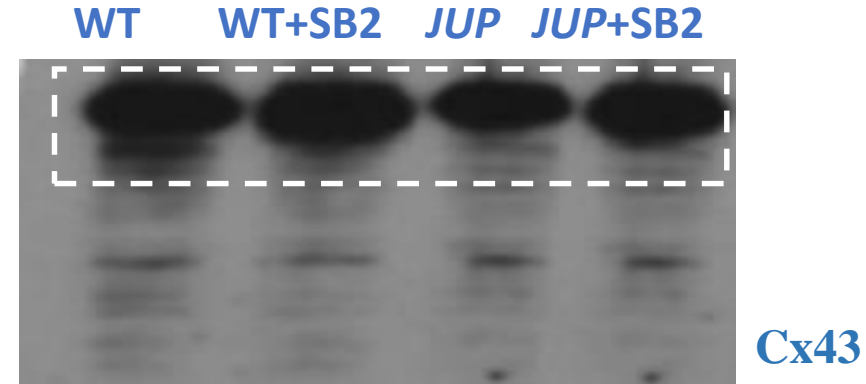
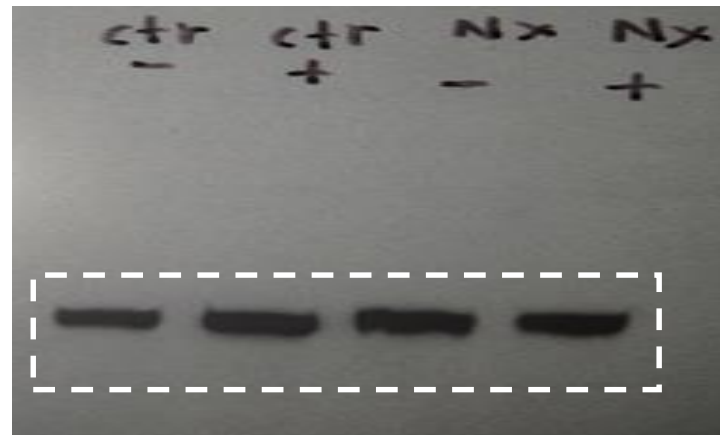
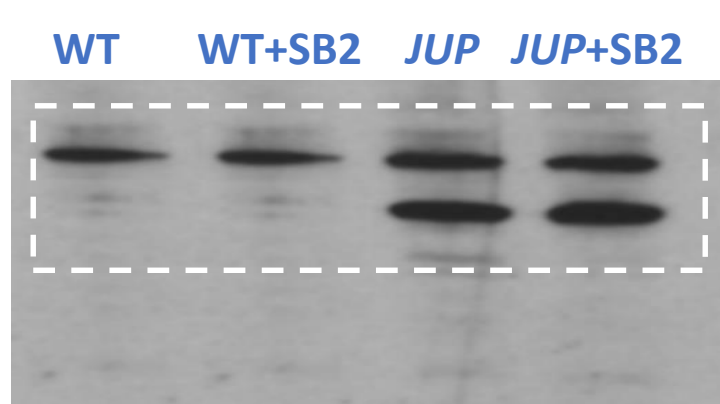


**GAPDH**



Full unedited gels for **Figure 5C** (*Dsg2* Mutant Mouse, Upper Panel)

# Full unedited gels for **Figure 5D** (*JUP* Mutant Mouse, Lower Panel)



WT *JUP*<sup>2157del2</sup> WT *Dsg2*<sup>mut/mut</sup>

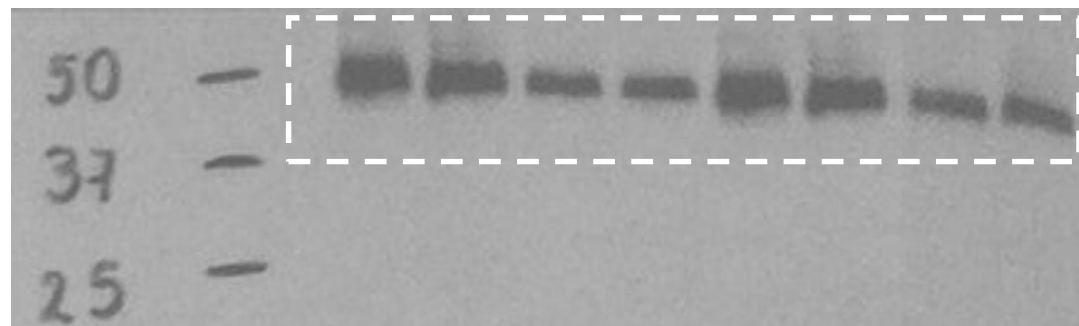
+

+

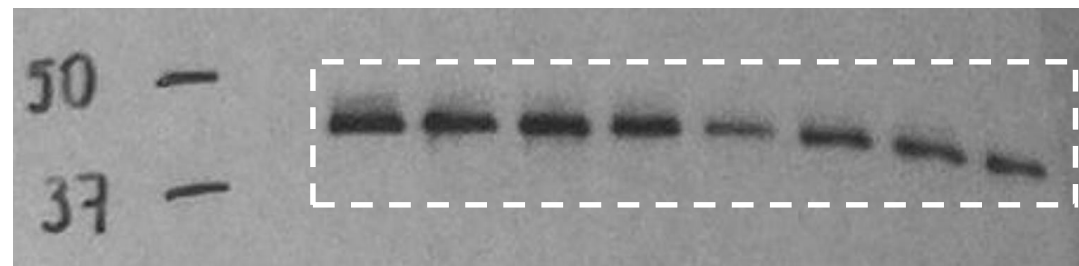
+

+

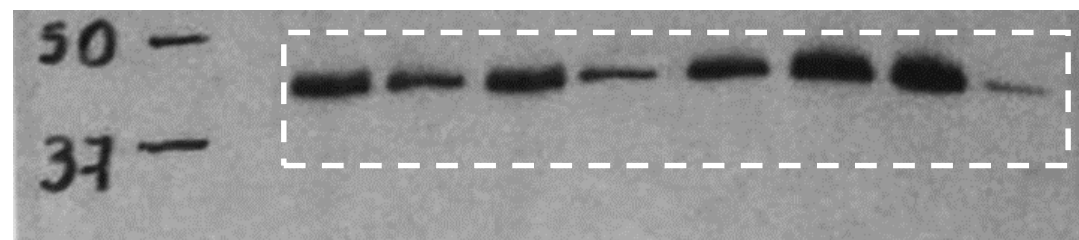
SB216763



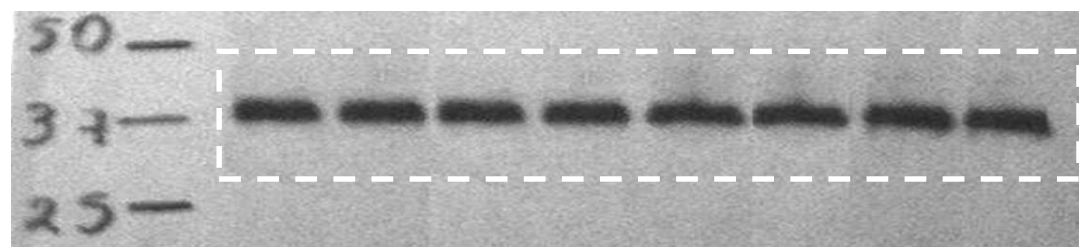
GSK3 $\alpha$



pGSK3 $\beta$  (Ser9)



GSK3 $\beta$



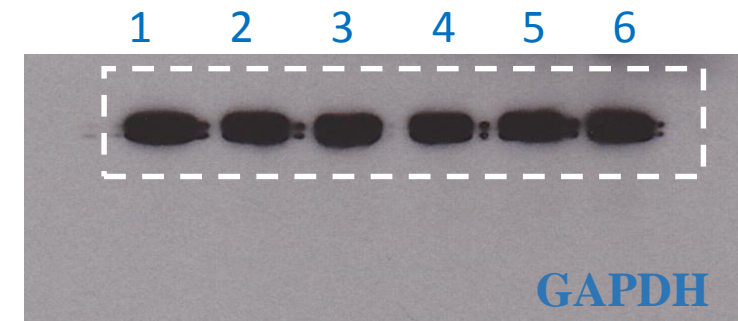
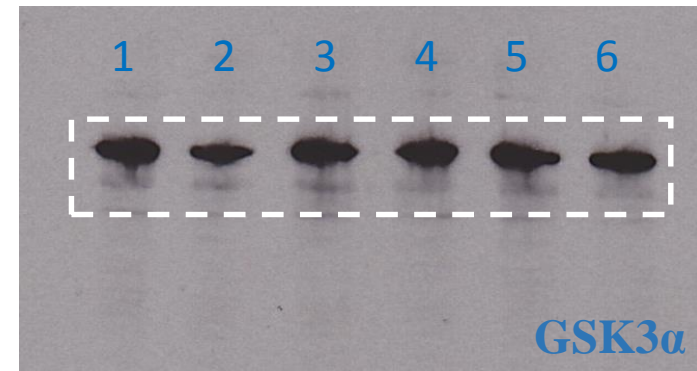
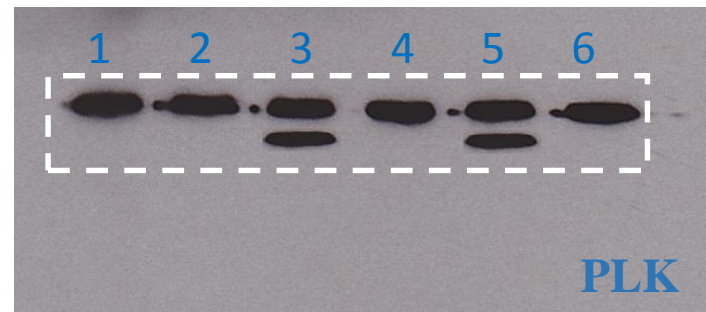
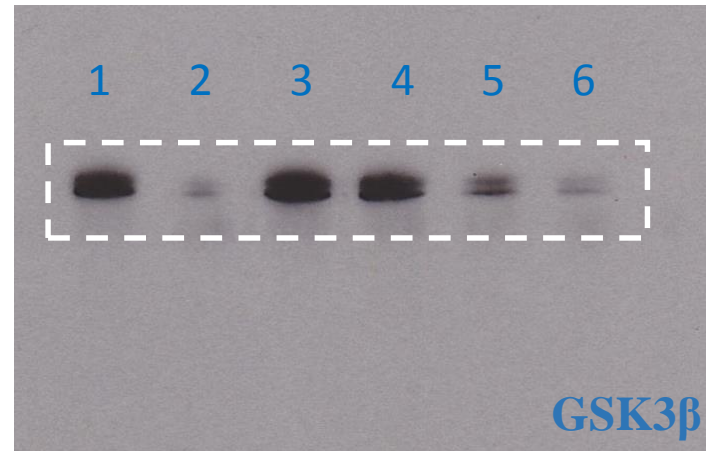
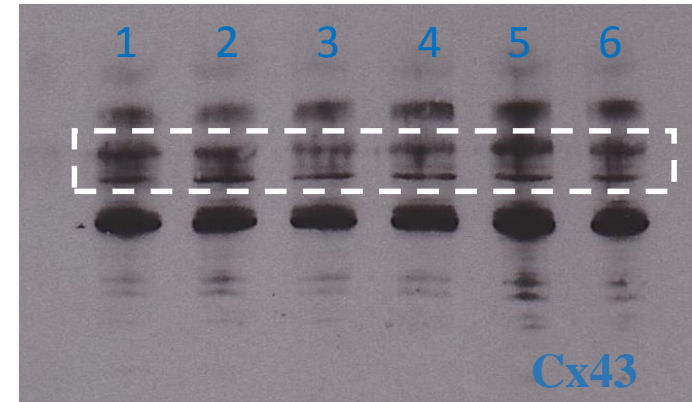
GAPDH

Full unedited gels for **Figure 6B**

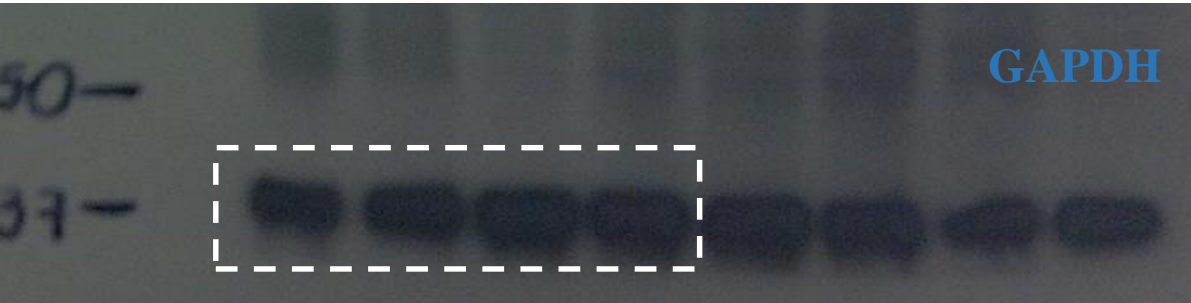
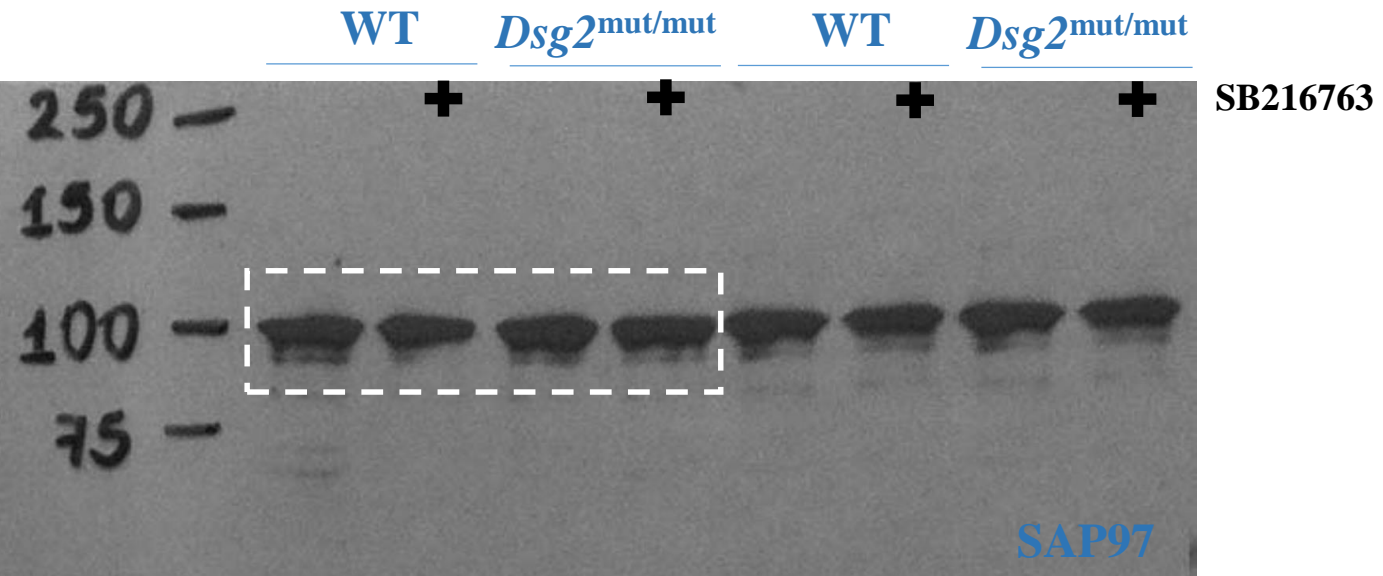


# Full unedited gel for **Figure 8A**

1. un-transfected controls
2. **GSK3 $\beta$ -shRNA**
3. ***JUP*<sup>2157del2</sup>**
4. ***PKP2*<sup>1851del123</sup>**
5. ***JUP*<sup>2157del2</sup> & GSK3 $\beta$ -shRNA**
6. ***PKP2*<sup>1851del123</sup> & GSK3 $\beta$ -shRNA**



# Full unedited gels for Supplementary Figure 3B



This is the same GAPDH film presented in Figure 5C, however this is the exact same blot that SAP97 was run on.

